Quest Journals
Journal of Research in Environmental and Earth Sciences
Volume 9 ~ Issue 4 (2023) pp: 156-172
ISSN(Online) :2348-2532
www.questjournals.org

Research Paper

Assessment and Prediction of Soil Moisture Index of Nepal Using Geospatial Techniques

Amit Tiwari [1,2], Bhawana Baniya [1], Ashish Dutta [1], Prajwol K.C. [1], Pradeep Gyawali [1,3,] Kutubuddin Ansari[4]

[1]*Department of Geomatics Engineering, Kathmandu University, Dhulikhel 45210, Nepal*
[2]*Devdaha Municipality, Government of Nepal, Khaireni, Rupandehi 32907, Nepal*
[3]*Head , Survey Office Darchula, Nepal*
[4]*Integrated Geoinformation (IntGeo) Solution Private Limited, New Delhi, 110025, India*

Abstract
The determination of soil moisture (SM) that directly affects agriculture productivity and brings uncertainty in climate change is crucial in Nepal because it's being an agricultural country. The main purpose of this study is to estimate the soil moisture index (SMI) of Nepal from 2012 to 2020 and predict the SMI for 2021. The relationship between Normalize difference vegetation index (NDVI) and land surface temperature (LST) from the Moderate Resolution Imaging Spectroradiometer (MODIS) satellite product was used for estimating the SMI for four seasons of the year 2012 to 2020 based on the universal triangle method. Rainfall data product from Climate Hazards Group InfraRed Precipitation with Station data (CHIRPS) was used for analyzing its relation with SMI. It depicts a positive relationship with SMI. The land cover map of the MODIS data product was used with SMI and analyzed at a period of four years as the land cover of the whole of Nepal doesn't drastically change over a year which is the study area. The result shows more SMI in the lower belt of Nepal i.e Terai region where vegetation is more than in other regions. This indicates a positive correlation between vegetation with SMI. SMI for the spring season of 2020 is predicted by feeding SMI values from the year 2012-2019 to the eps-regression model as a training sample and the year 2020 as a testing sample. Statistical evaluation such as RMSE, MSE, MAE, and R-squared test was conducted in actual and predicted SMI values of the year 2020. SMI is predicted for the spring season of the year 2021 using the tested and validated model. This paper contributes to a better knowledge of SM dynamics around Nepal, which can aid in agriculture's improvement and the SM assessment/prediction and can be used to detect early indicators of drought, for decision-making weather forecasting, or any national research objective.

Keywords: *Soil Moisture; MODIS; LST; NDVI; CHIRPS; Universal Triangle Method*

Received 12 Apr., 2023; Revised 25 Apr., 2023; Accepted 27 Apr., 2023 © *The author(s) 2023. Published with open access at www.questjournals.org*

I. Introduction

According to the Ministry of Agriculture and Livestock Department 2018, Nepal is an agriculturally driven country with 66% livelihood based on agriculture[1,2] Agriculture is the major source of food security and income which alleviate poverty and uplift living standards. It also contributes to the growth, social welfare, and human development of the general people of Nepal [3]. Nepal's poverty-reduction initiatives and economic growth are largely driven by the expansion of its agriculture sector, which accounts for one-third of the country's Gross Domestic Product (GDP) [4]. As a large sum of the population is dependent on agriculture for their livelihood, improving the agricultural status of Nepal will bring a significant positive change in the overall development of people diminishing poverty and ensuring food security.

Nepal has various types of ecological zones like plains, hills, and mountains where farming is done according to different seasons i.e summer (June to August), winter (December to February), spring (March to May), and autumn (September to November) [5]. As climate change has been observed in this country [6], it is a major factor affecting Nepal's agriculture recently. Climate change-related drought has emerged as a cause of household-level vulnerability in Nepal's agriculture. Climate change affects the temperature pattern, precipitation patterns and can cause extreme weather events which will then affect water availability causing lower agricultural production. Soil Moisture (SM) is one fo the factors that affects agricultural productivity and

is affected by climate change which is why assessing and analyzing SM is important for Nepal. SM is the water content of the soil which is affected by different soil types, climate, topography, vegetation, and other variables. SM influences the chemical, physical and biological characteristics of the soil [7]. Agriculture production is heavily dependent on SM. Lack of SM can result in a significant amount of loss in crop production [8]. Although Nepal has a large population dependent on agriculture, this vital issue of SM measurement has not been taken into consideration as a significant study topic. According to Talchabhadel et al. [9] the study concerning SM for Nepal is very limited. A precise estimation of soil moisture content (SMC) is important for soil water balance calculations, various hydro-meteorological, ecological, or biogeochemical modelling applications, and initialization of varied land-atmosphere models. Estimating SMC is crucial for many water budgeting processes and meteorological and agricultural applications [9].

The soil moisture index (SMI) is defined as the proportion of the difference between the present SM and the permanent wilting point to the field capacity and the residual SM. The index values range from 0 to 1 where 0 indicates extreme dry conditions and 1 indicates extreme wet conditions [10]. SM can be assessed in two ways in-situ and Remote Sensing (RS) methods. Insitu measurement provides the most accurate SM measurement however it is an extremely tedious process that is expensive and time-consuming [11]. It suits a small area over a small period [10]. However, not optimal for rapid and continuous SM monitoring at the regional scale. For SM estimation of the large spatial extent, RS methods are best because of their large coverage, continuous, and easily available data. RS measurements from Terra/Aqua Moderate Resolution Imaging Spectroradiometer (MODIS) have been used for the SM estimation. Even though another source of RS like Sentinel data product has high-resolution data, MODIS is preferred as sentinel products don't provide enough coverage and continuous data for the whole of Nepal over a long period. Nepal being a developing and geographically diverse country does not have many resources for in-situ measurement of the whole of Nepal. Thus, RS methods using MODIS data product is used for the urgent need of measurement and prediction of SMI for better agricultural practice and management decisions [9]. Price (1990) first proposed the triangle concept, which was further expanded upon by Carlson et al. (1994; 1995) and Gillies and Carlson (1995) for SM estimate using Land Surface Temperature (LST) and normalized difference vegetation index (NDVI) [12]. Researchers like Wang et al. [13], and Yang et al. [9] have used the universal triangle method for estimating SMI. SM has a complicated relationship with NDVI and LST [14].

Given the importance of SM for a geographically diverse agrarian Nepal, RS-based SMI can be used for the comprehensive understanding of SM response to rainfall from a rapidly changing climate. The understanding of changes in SM with different land cover types eases conducting agricultural planning and other soil-related activities. Knowing the future state of the soil moisture would be great for reservoir management, early drought warning, irrigation scheduling, and crop production forecasting [15]. Predicting soil moisture can serve many other purposes than just agriculture for which different methods can be used. Artificial neural network (ANN), Naive Bayes algorithm, Support vector machine (SVM) are some of the prediction methods [16–18]. Predicting SMI of whole Nepal with certain time restrictions gives us limited choice from available predicting methods. Support vector machine (SVM) is stable and it surpasses other algorithms in terms of accuracy and prediction speed [19]. SVM also uses less memory and performs analysis in a multidimensional dataset to classify [20].

In this study, the soil moisture index of the entire of Nepal is assessed and analyzed. The main objectives of this study are: (a) to estimate the SMI of Nepal from the year 2012 to 2020 using MODIS products, (b) to show the variation in SMI with land cover types, (c)to show the variation of SMI in geographical region and season, and (d) to show the relationship between SMI and rainfall, and (e) to predict SMI of the year 2021 using SVM and historical data. To the best of our knowledge, this is the first study for Nepal that uses MODIS products to predict future SMI for the country and validate at a local level. This paper contributes to a better understanding of SM, which can aid in improving agriculture and its sustainable development. This process of SM assessment and prediction can be useful in developing countries like Nepal for SM assessment/prediction which can be used to detect early signs of drought, weather forecasting for decision making, or any research purpose at a national level.

II. Materials and Methods

2.1 Study Area

Nepal is an agriculturally driven country, with Himalayan, Hilly, and Southern Terai plains. Terai has high vegetation, also known as the 'breadbasket' of Nepal and the Himalayan region has very low vegetation. It lies between two big countries like India in the south and China in the north and has an 80°4' and 88°12' East longitude and 26°22' and 30°27' North latitude with a total area of 147,516 square kilometres. The entire distance from east to west is about 800 km while from north to south is only 150 to 250 km. Nepal has vast water systems that drain south into India. The country can be divided into three main geographical regions: the Himalayan region, the Hilly region, and the Terai region. The elevation values range from 59 meters in tropical

Terai to 8848 meters in the Himalayan. The major altitude belts of Nepal are Tropical Zone (below 1000 meters), Subtropical Climate Zone (1,000 to 2,000 meters), Temperature Climate Zone (2,000 to 3,000 meters), Subalpine Zone (3,000 to 4,000 meters), and Alpine zone (4,000 to 5,000 meters). In this project, the season of Nepal has been categorized into 4 seasons such as spring (March-May), summer (June-August), autumn (September-November), and winter (December-February).

In recent years the rapid climate change has affected the agriculture productivity of Nepal [2]. The growth of the agriculture sector was limited to 2.9% during the last decade, whereas the growth rate of the agricultural sector in recent years is found at 2.8% only, which indicates a low rate [1]. This is because agriculture is heavily affected by unlikely climate and floods/drought. Since agriculture is a primary source of income and food security, it is important to improve the agriculture system and production.

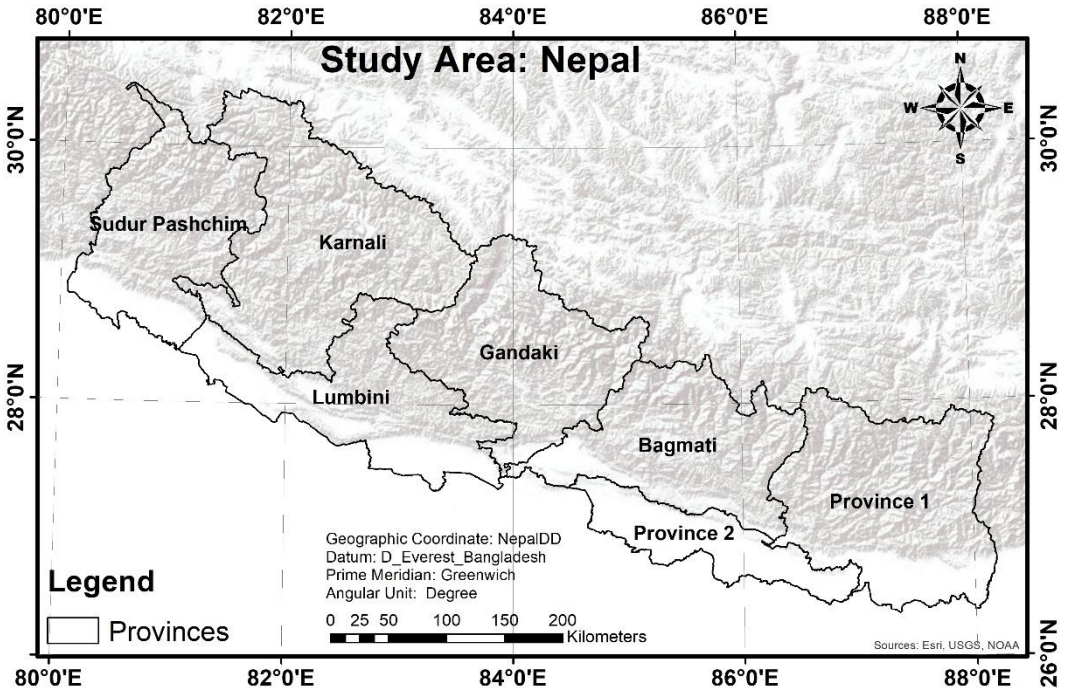

Figure 1. Location map of Nepal as a study area.

2.2. Data

2.2.1. MODIS Products

The Moderate Resolution Imaging Spectroradiometer (MODIS) is a primary instrument onboard the Earth Observing System (EOS) Terra and Aqua platforms that use a range of visible, NIR, MIR, and thermal channels to monitor the Earth's atmosphere, ocean, and land surface [21]. The MODIS data product we used are listed below:

1. NDVI quantifies vegetation by measuring the difference between near-infrared (which vegetation strongly reflects) and red light (which vegetation absorbs) as in equation 1:

$$NDVI = \frac{(NIR - Red)}{(NIR + Red)}, \quad (1)$$

where NIR is near-infrared spectral reflectance and Red is visible red spectral reflectance. It always ranges from -1 to +1. But there isn't a distinct boundary for each type of land cover [22]. Healthy vegetation (chlorophyll) reflects more near-infrared (NIR) and green light compared to other wavelengths. But it absorbs more red and blue light. Unhealthy plants reflect higher red resulting in lower NDVI. The earth science data type for MODIS NDVI is MOD13A2. It is a sixteen-day compositing period. It provides Vegetation Index (VI) values at a per-pixel basis at 1 kilometer (km) spatial resolution [23]. Image data of the year 2019 are shown.

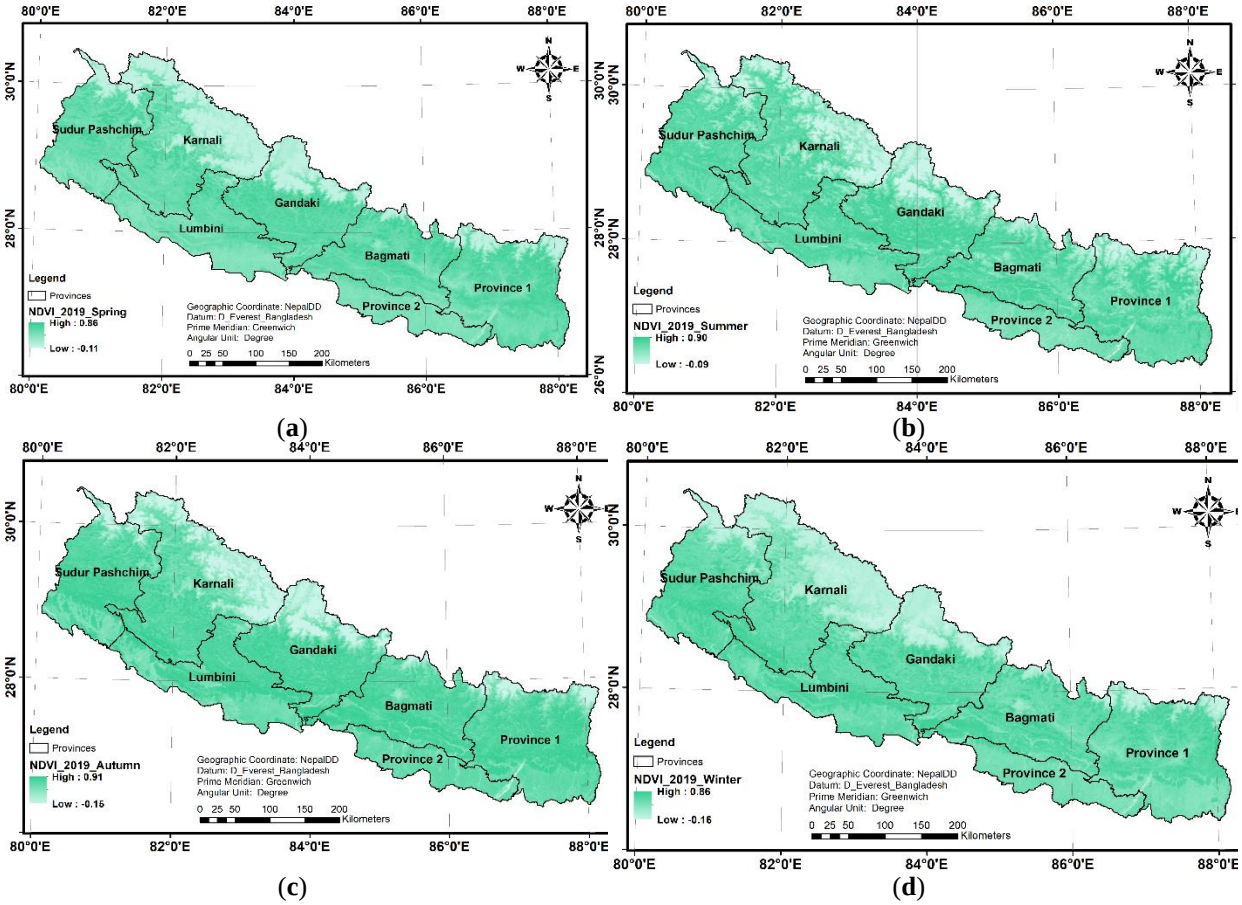

Figure 2. Normalized Difference Vegetative Index (NDVI) map of Nepal 2019 (**a**) Spring, (**b**) Summer (**c**) Autumn and (**d**) Winter.

2. LST is an important parameter for environmental studies and enables the monitoring of landscape processes and responses, such as the surface energy and water balance [24]. It is the temperature of the skin surface of land which can be derived from the satellite information or direct measurements in the remote-sensing terminology [25]. The earth science data type for MODIS LST is MOD11A2. It is an eight-day compositing period. It provides values at a per-pixel basis at 500 meters (m) spatial resolution. It was chosen because twice of such period is the exact ground track repeat of the Terra Platform. LST over eight days is the average LSTs of the MOD11A1 product over eight days.

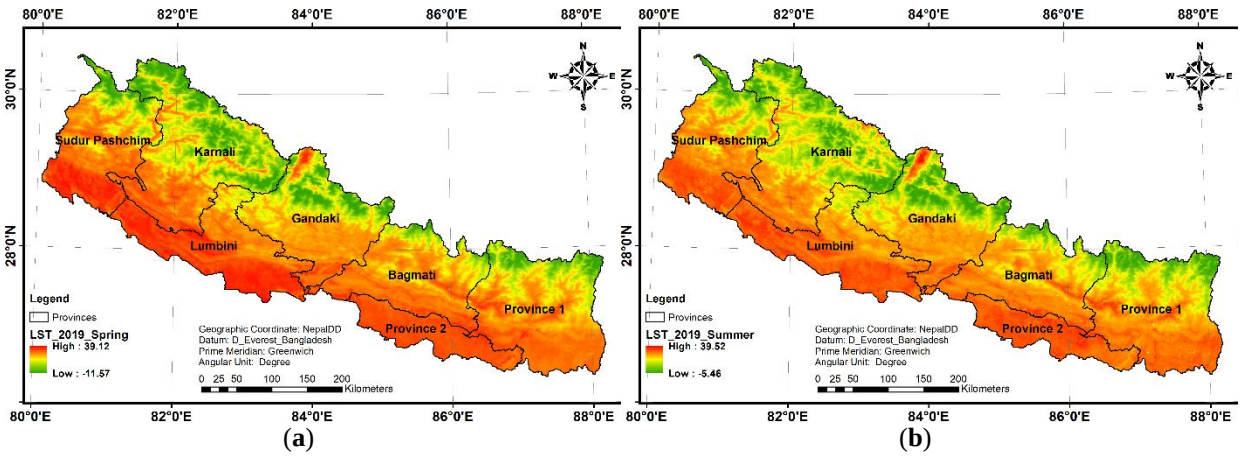

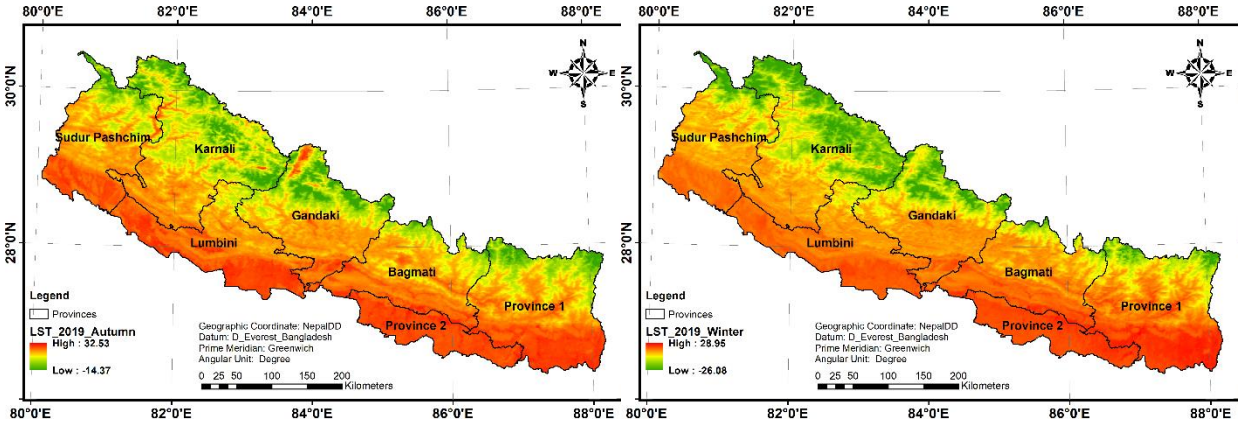

Figure 3. Land Surface Temperature (LST) map of Nepal 2019 (**a**) Spring, (**b**) Summer (**c**) Autumn, and (**d**) Winter.

3. Land Cover implies the physical or natural state of the Earths' surface. Land cover maps represent spatial information on different types (classes) of physical coverage of the Earth's surface, e.g. forests, grasslands, croplands, lakes, wetlands [26]. It represents how much of a region is covered by the mentioned land cover types.

The MODIS Land Cover Type Product (MCD12Q1) provides a suite of science data sets (SDSs) that map global land cover at the 500-meter spatial resolution at the annual time step for different land cover legends. The maps were created from classifications of Spectro-temporal features derived from data from the MODIS. MCD12Q1 contains 13 science data sets, among which This product is created using the supervised classification of MODIS reflectance data for which Land Cover Type 1 (LC_Type1) was used.

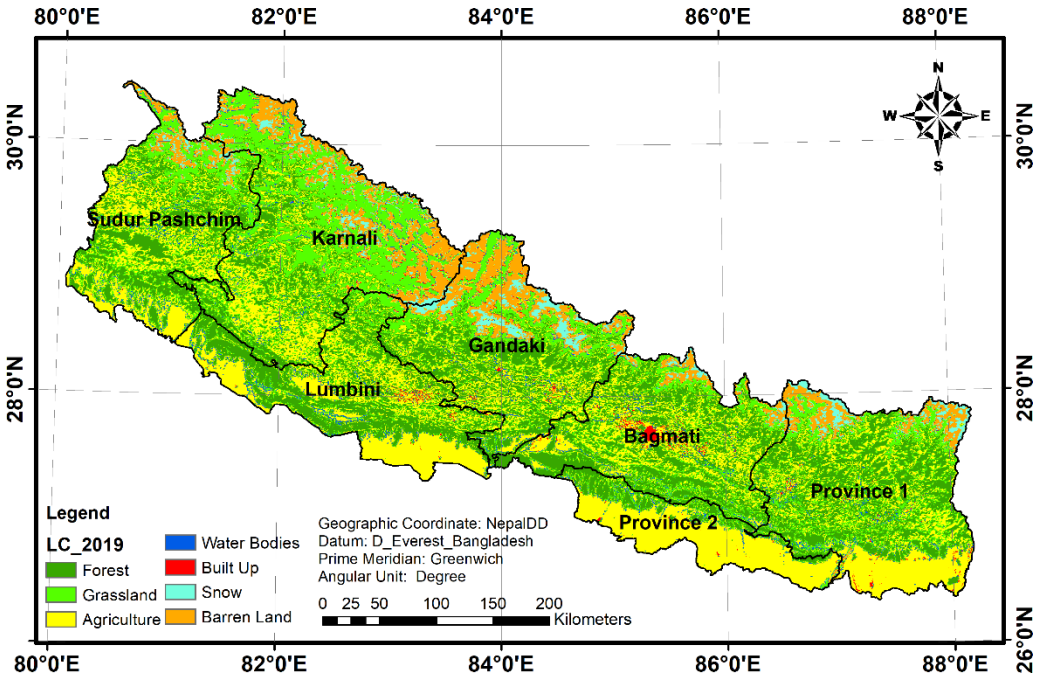

Figure 4. Land Cover map of Nepal 2019.

2.2.2. CHIRPS Data

As rainfall plays an important role in SM, rainfall data are downloaded from Climate Hazards Group InfraRed Precipitation with Station data (CHIRPS). CHIRPS is a quasi-global rainfall data set that spans 35+ years. CHIRPS combines 0.05° resolution satellite images with in-situ station data to construct gridded rainfall time series for trend analysis and seasonal drought monitoring, spanning 50°S-50°N (and all longitudes) from 1981 to near-present [27]. CHIRPS was developed to provide complete, reliable, and up-to-date data sets for a variety of

reasons in aid for research and analysis [28]. The monthly composited data are downloaded. These monthly composite data are then made a composite of three months.

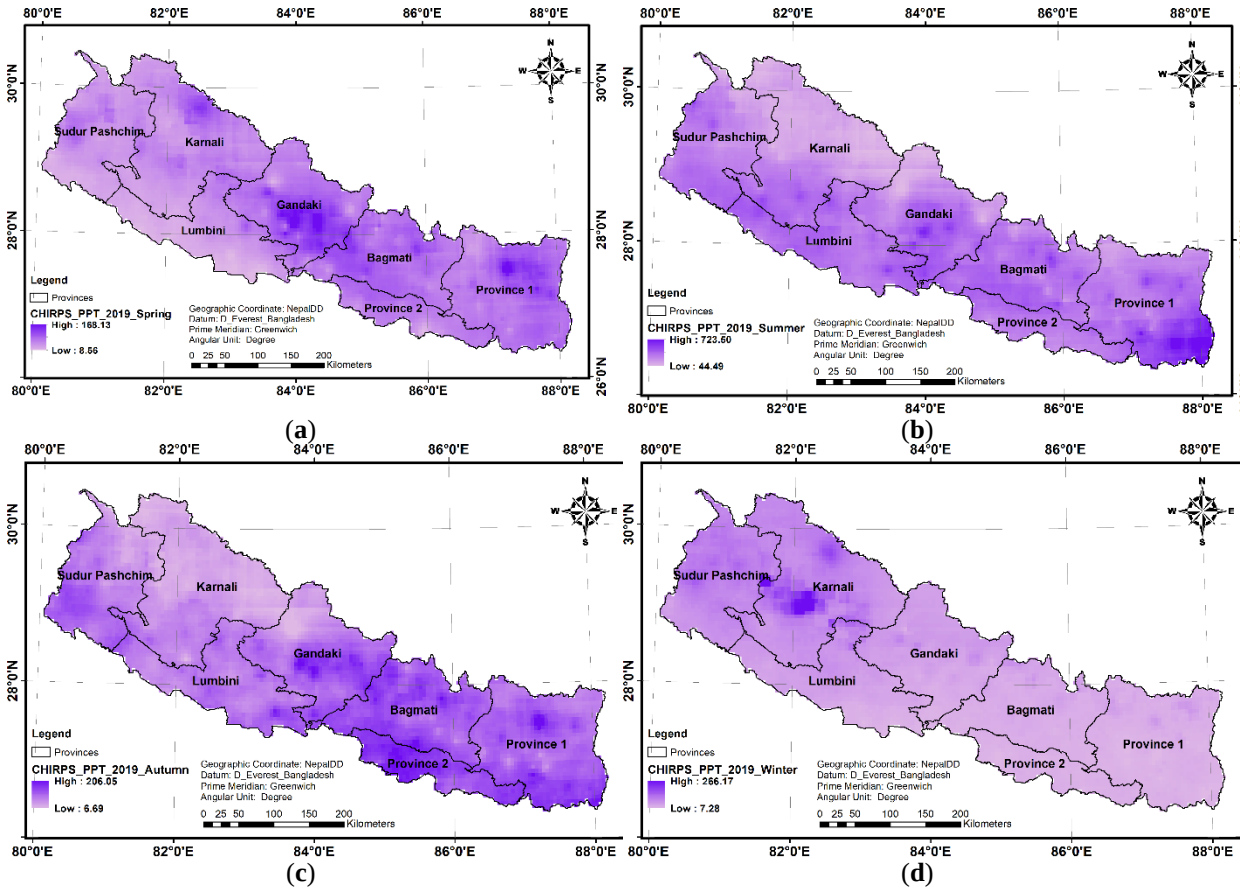

Figure 5. Rainfall map of Nepal 2019 (**a**) Spring, (**b**) Summer (**c**) Autumn, and (**d**) Winter.

2.3. Methodology

The MODIS images of LST, NDVI from 2012-2020, and Land Cover images of 2015 and 2019 were downloaded from the official USGS database. The criteria while downloading images were 10% cloudy. The obtained image of LST, NDVI, and Land Cover was converted to WGS1984 from sinusoidal projection using the HDF-EOS to GeoTIFF Conversion Tool (HEG) tool. Then, for LST and NDVI composite of 96 days was done. MODIS Land Cover maps were created from classifications of spectro-temporal features. It was created by using the supervised classification of MODIS reflectance data. Here, Land Cover Type 1 (LC_Type1) was used which is categorized into seven different groups i.e., Forest, Grassland, Agriculture land, Barren land, Built-up area, snow, and water bodies. Rainfall data images were downloaded from CHIRPS from the year 2012-2020 making a composite of 3 months.

The LST and NDVI values were generated for the respective seasons of the respective year. Along with this, LST, NDVI, LC, and Rainfall maps were prepared. A Scatter plot between LST and NDVI was generated which was used for assessing SMI based on the Universal Triangle method. The dry edges and wet edges were then generated from a scatter plot. Using the coefficients of dry edge and wet edge from the scatter plot, SMI was generated in TIFF format. Similarly, SMI maps were created from the year 2012 to 2020 for four seasons' i.e., winter, autumn, spring, summer. For validation of produce SMI maps, sentinel image (SMAP_L2_SM_SP) of the year 2015 and 2016 spring was used. For the evaluation of the model, statistical evaluation such as RMSE, MSE, MAE, and R-squared test was conducted.

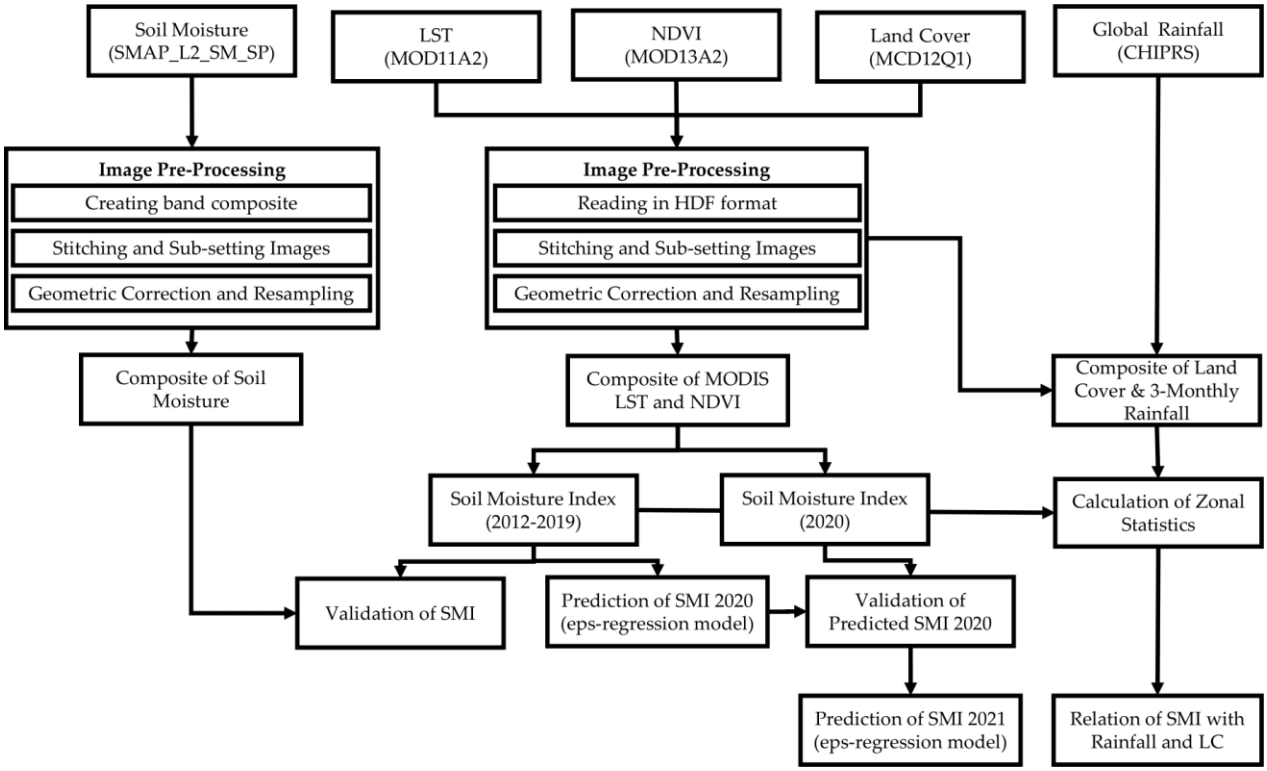

Figure 6. The workflow of the study.

Two land cover maps of the years 2015 and 2019 were created for the analysis of their relationship with SMI. Rainfall maps are created from 2012 to 2019 of whole Nepal for analysis of its relationship with SMI. After the validation of SMI maps the zonal statistics tool was used to analyze the values obtained. The analysis of region-wise seasonal variations of SMI with the land cover map was done and the relationship of rainfall and soil moisture was derived from 2012 to 2019. From the estimated SMI maps from the year 2012 to 2019 a model was created using SVM to predict the SMI of 2020 and after the model was validated from the estimated 2020 map, the same model was for the prediction of the 2021 SMI maps. For the prediction of the SMI value of the year 2021, the evaluated SMI values of the year 2012-2020 were used. A support vector regression model was used for the prediction of SMI values under the R package "e1071". The training/testing partitions of the SMI values were created using the createDataPartition() method which was available under the "caret" package. For the evaluation of the model, statistical evaluation such as RMSE, MSE, MAE, and R-squared test was conducted in actual and predicted SMI values of the year 2020.

2.3.1. Universal Training Method

Data analysis revealed a distinct relationship, sometimes referred to as the "Universal Triangle," between soil moisture (SM), the normalized difference vegetation index (NDVI), and LST for a given region [12]. Figure 7 represents a schematic description of the relationship referred to as the "Universal Triangle.".

The line from point A to point C in Figure 7 represents the driest conditions, namely "dry edge", under different vegetation coverage. The line from point B to point D in Figure 7 represents the wettest conditions, namely "wet edge", under different vegetation coverage. Ts is positively correlated with NDVI along the wet edge (from point B to point D) and negatively correlated with NDVI along the dry edge (from point A to point C).

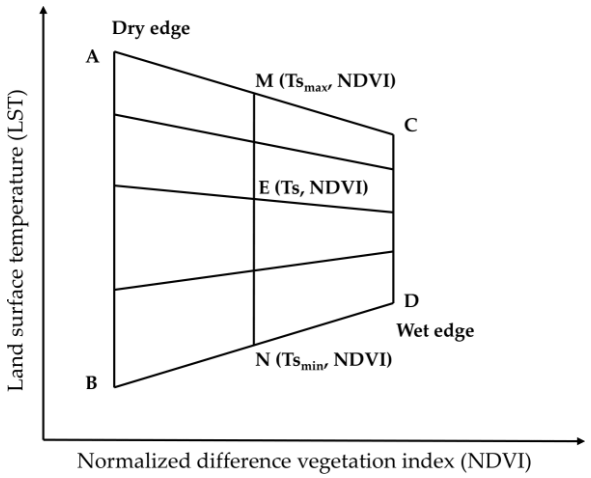

Figure 7. The plot in LST- NDVI space and the definition of SMI [29].

SMI can be assessed by the parameters derived from figure 7:

$$\text{SMI} = \frac{\text{Tsmax} - \text{Ts}}{\text{Tsmax} - \text{Tsmin}} \qquad (2)$$

Where, Tmax, Tmin is the maximum and minimum surface temperature for a given NDVI. Ts is the remotely sensed data-derived surface temperature at a given pixel for a given NDVI.

$$Tsmax = a1 * NDVI + b1 \qquad (3)$$

$$Tsmin = a2 * NDVI + b2 \qquad (4)$$

Here, in equations (3) and (4), the parameters a1, a2, and b1, b2 are empirical parameters that are obtained by linear regression of known remotely-sensed data for both the dry and wet edges [14].

2.3.2. Support Vector Regression

Support vector regression (SVR) works on the principle of SVM and is the counterpart of SVM for the regression problems. SVMs have supervised learning models with associated learning algorithms that analyze data used for classification and regression analysis. SVR has been used in several fields due to its high prediction accuracy and ease of modelling. SVM is a set of related supervised learning methods used for classification and regression analysis. In the early 1990s, Vapnik et al. created SVMs for classification applications. Later, Vapnik (1995) expanded on his work by developing SVMs for regression [18]. SVM also possesses the well-known ability to be universal approximators of any multivariate function to any desired degree of accuracy [30]. It has been found that SVMs show better or comparable results than the outcomes estimated by neural networks and other statistical models [31]. SVMs are applied in statistics, computing, and other fields with great success. Pasolli et al. [32] predicted the SM using the support vector regression model.

2.3.3. Validation

Validation is aided by various criteria for evaluating and determining model parameters. In this study, validation was performed in two different stages. The first was the verification of the estimated SMI. The second step was the validation of the predicted SMI. The parameters employed for evaluation here are: the correlation coefficient (R), root-mean-square error (E_{RMS}), and mean absolute error (E_{MA}).

A sentinel image with the product name SMAP L2 SM SP was used for SMI validation. For validation, images of the years 2015 and 2016 of the spring season were used. Statistical model evaluations such as E_{RMS}, E_{MA}, E_{MS}, and R-squared tests were undertaken in the actual and expected SMI values of the year 2020 for the validation of predicted SMI. an equation:

$$E_{MA} = \frac{\sum_{i=1}^{n} |y_i - y_i^*|}{n}, \qquad (5)$$

$$E_{MA} = \frac{\sum_{i=1}^{n} (y_i - y_i^*)^2}{n} \qquad (6)$$

$$E_{RMS} = \sqrt{\frac{\sum_{i=1}^{n} (y_i - y_i^*)^2}{n}}, \qquad (7)$$

$$R^2 = 1 - \frac{\sum (y_i - y_i^*)^2}{\sum (y_i - \overline{y})^2}, \qquad (8)$$

where n is the number of samples, y_i, y_i^* and $\overline{y}$ are measured, predicted, and mean values respectively. The smaller the E_{RMS} and E_{MA} are, and the larger R –the square is, the better the model performs. The model is considered viable if R is not less than 0.5 [33].

III. Results and Discussion

3.1 Relationship between LST and NDVI

The scatter plotter between LST and NDVI values for the respective season of the respective year was obtained. The scatter plot (Figure 8) shows many points. Each point represents the values of these two variables. The scatter plot formed by LST and NDVI forms like a triangle. The upper edge of the triangle is defined as a dry edge (Figure 9) and the lower one is a wet edge (Figure 10). After that, dry edges and wet edges are generated we get empirical parameters (a1, b1, a2, and b2) by linear regression, and using these parameters of dry edge and wet edge (Table 1) from the scatter plot SMI was calculated. Thereafter, soil moisture index in TIF formats was generated.

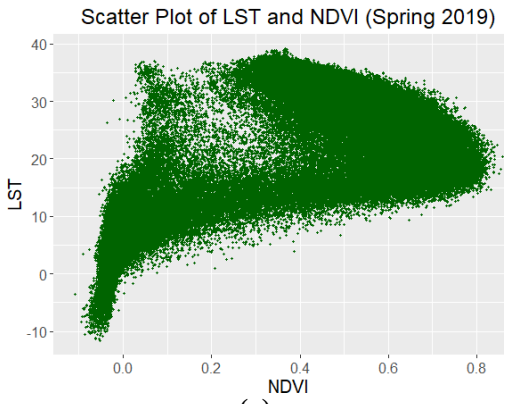

(**a**)

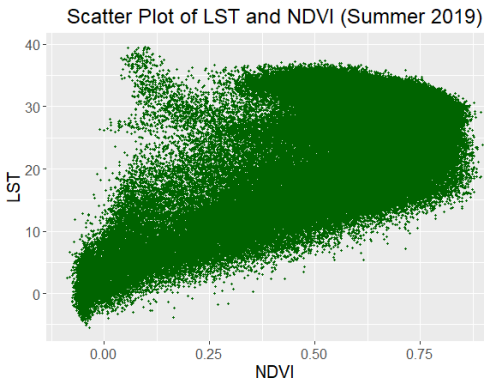

(**b**)

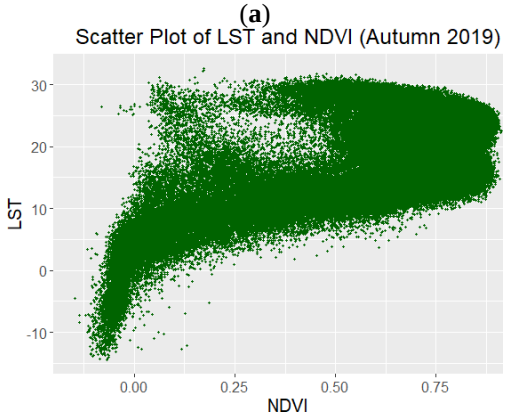

(**c**)

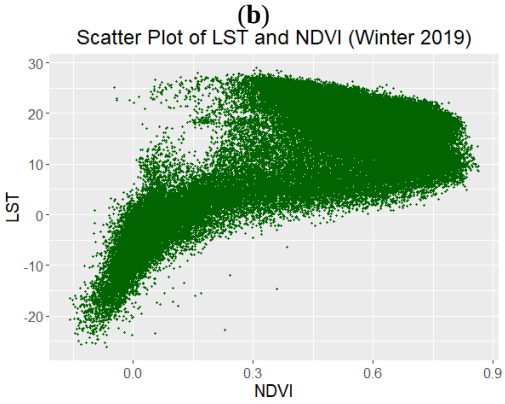

(**d**)

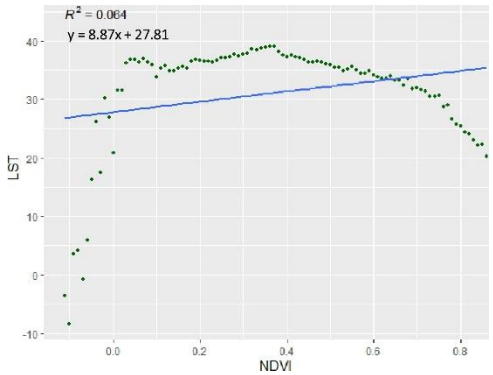

(**a**)

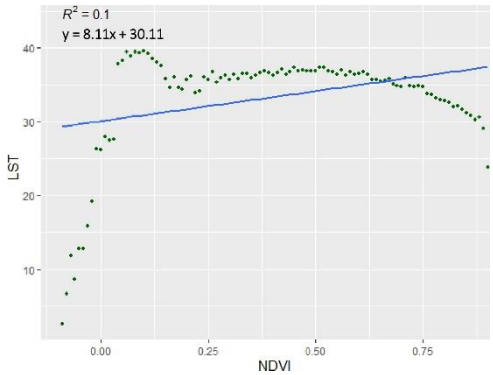

(**b**)

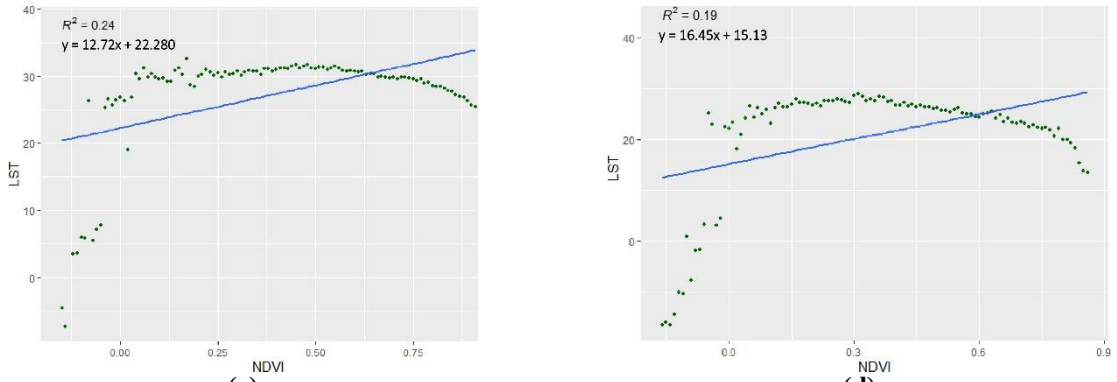

(**c**) (**d**)

Figure 8. Scatter plot of LST and NDVI of Nepal 2019 (**a)** Spring Season, (**b**) Summer Season, (**c**) Autumn Season, and (**d**) Winter Season.

Figure 9. Dry Edge of the year 2019 (**a**) Spring Season, (**b**) Summer Season, (**c**) Autumn Season, and (**d**) Winter Season.

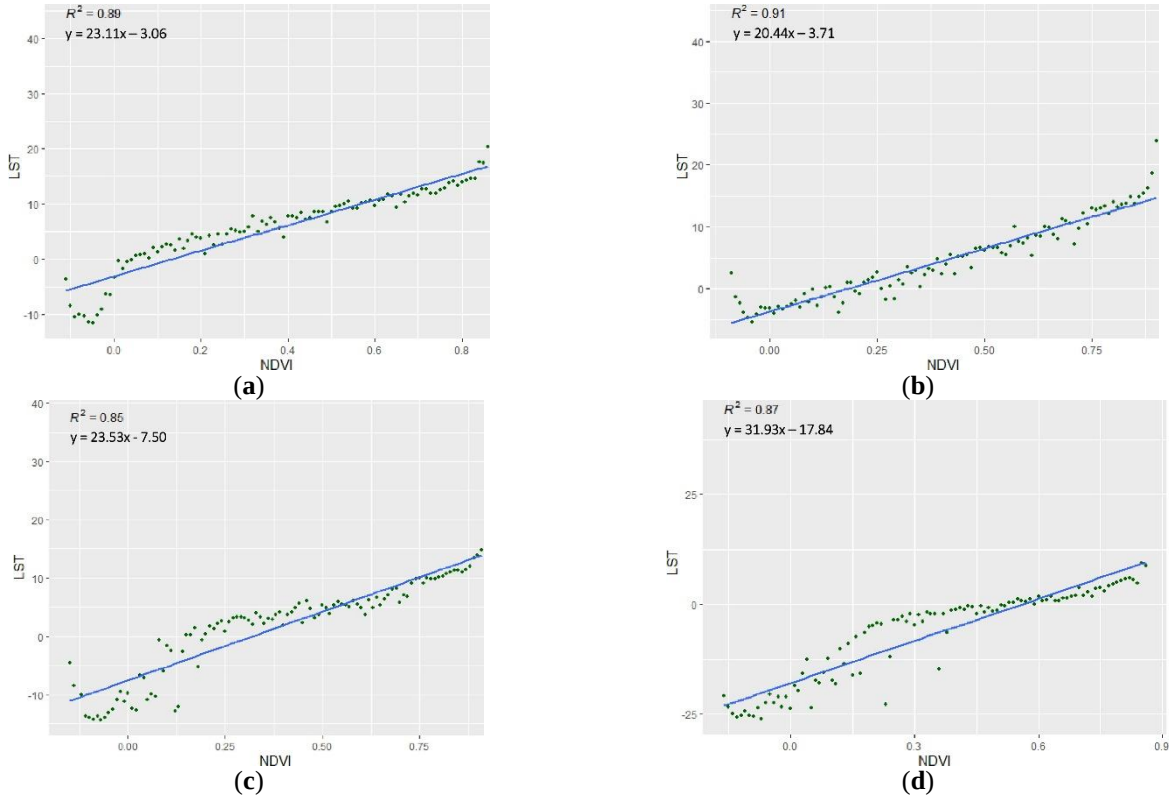

(**a**) (**b**)

(**c**) (**d**)

Figure 10. Wet Edge of the year 2019 (**a**) Spring Season, (**b**) Summer Season, (**c**) Autumn Season, and (**d**) Winter Season.

Table 1. Parameter of the dry and wet edge of the year 2019 (a1, b1 are the parameter for dry edge and a2, b2 are the parameter for wet edge).

Seasons	**a1**	**b1**	**R^2**	**a2**	**b2**	**R^2**
Spring	8.872	27.809	0.064	23.11	-3.06	0.89
Summer	8.113	30.112	0.10	20.438	-3.709	0.91
Autumn	12.72	22.28	0.24	23.53	-7.498	0.85
Winter	16.45	15.13	0.19	31.93	-17.84	0.87

1

3.2. Soil Moisture Index (SMI) Maps

Different seasonal SMI maps were prepared. Yearly, the SMI gradually decreases. Mostly, SMI is high in the Terai region and low in the Himalayan region as shown in Figure 11. The SMI of the Terai region is more than the Hilly and the Himalayan region. The SMI of the Hilly region is less than the Terai but more than the Himalayan region and the SMI of the Himalayan is less than both the Terai and the Hilly region. But in mustang, SMI is high. The possibilities of this are soil type and percolation capacity index. The soil in mustang is a slit that comes under course texture soil. Such soil texture didn't show a great relationship with the reflectance values. The soil percolation rate indicates how quickly water moves through soil and helps evaluate the ability of the soil to absorb and treat effluent.

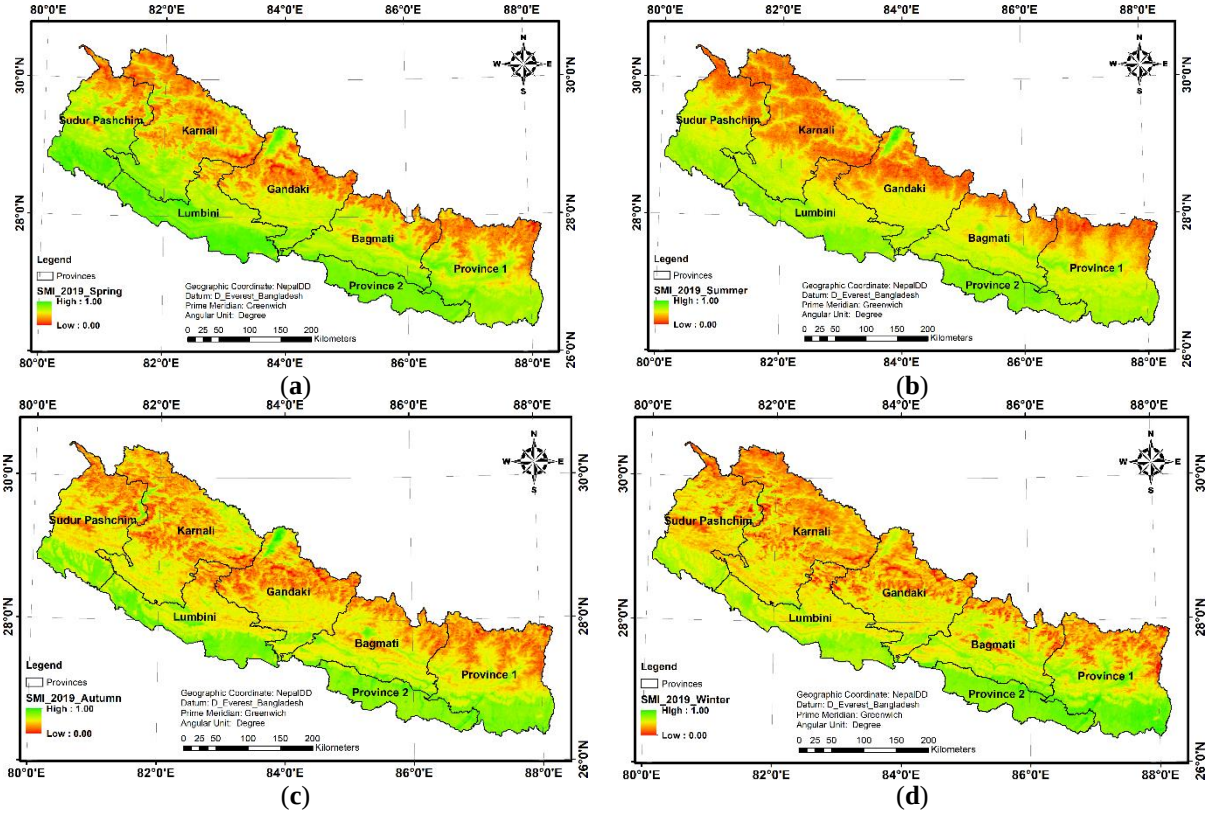

Figure 11. Soil Moisture Index (SMI) Map of Nepal (2019) (a) Spring (b) Summer (c) Autumn and (d) Winter.

3.3. Validation

For validation, a sentinel image (SMAP_L2_SM_SP) was used. The images of the 2015 and 2016 springs were used (Figure 12). The RMSE estimated was 0.2985, the mean square error was 0.1106 and the mean absolute error is 0.2621 for image 2015 spring. Similarly, the RMSE estimated was 0.034, the mean square error was 0.0012 and the mean absolute error was 0.0264 for image 2016 spring which was acceptable values.

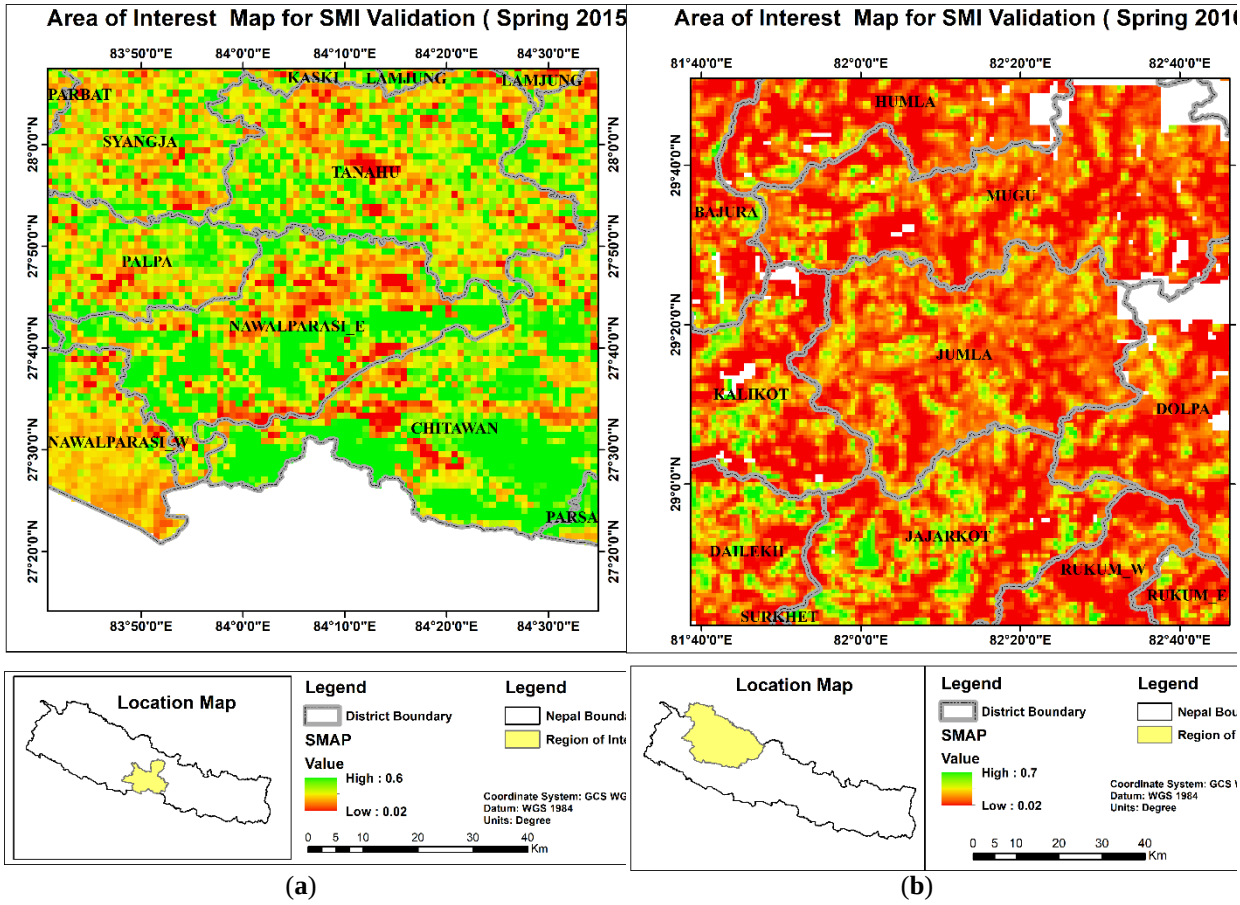

(**a**) (**b**)

Figure 12. Area of Interest Map for SMI Validation (**a**) Spring of the year 2015 and (**b**) Spring of the year 2016.

3.4. Seasonal Variation of NDVI and LST across Nepal

The variations of NDVI in different seasons across shows that the general vegetation seems high from mid-spring to summer i.e. from May to August with an average of 0.66 NDVI all across Nepal. The Terai and the Hilly are highly vegetated, the vegetation seems high in the lower belt of Nepal i.e. the Terai, and low in the upper i.e. the Himalayan region. Vegetation shows a negative relationship with temperature. However, vegetation isn't solely related to the temperature but with several factors, altitude, and soil type being one of them. LST differs from season to season and place to place. The temperature, in general, was high in summer i.e. June to August all over Nepal with an average temperature of 25.6 degrees Celsius. The temperature in Nepal was highest in the Terai with an average of 28.0-degrees Celsius and lowest in the Himalayas with an average of 2.0 degrees Celsius.

3.5. Comparing SMI with Land Cover Types

For analyzing the relationship between SMI and different landcover, landcover maps of 2015 and 2019 were created. The average pixel value of different land cover types like agriculture, barren land, built-up area, forest, grassland, snow, and waterbody was analyzed with the average pixel value for SMI as shown in Figure 13. The SM in the agricultural land, forest, water bodies seems high which is reasonable. The water content of the soil of the water body, the agricultural land, and the forest was high. From the chart (Figure 13), the agriculture, waterbody, forest, grassland, barren land, and snow area have gradual changes in SMI which are in agreement with Feng research and Yang research [9,34].

Our study is based on RS, it is highly dependent on the signal and its reflectance. Different surface types have different absorption and reflectance within a pixel. This explains the built-up having high SM because the built-up area has overlapping spectral reflectance. Due to this also, the SMI of the built-up area is seen as high. The infiltration rate and permeability also play role in this section. As a result, it is preferable to remove the built-up area in this technique since the soil moisture content of the built-up region is higher than that of other areas.

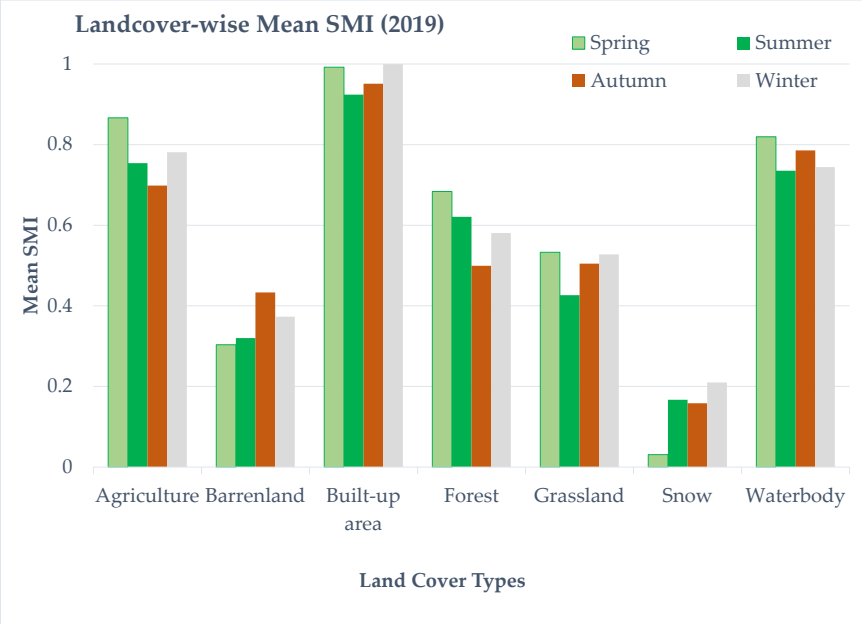

Figure 13. Land Cover-wises mean SMI (2019).

For reflecting the land covers and their variety in SM over seasons this analysis was carried out in particular years. There was no significant change in land cover over a small period so a period of 4 years was considered for the analysis. In 2015 and 2019, the graph shows that in snow land the SM seems low overall seasons whereas the SM in agricultural areas seems high after removing built-up areas.

The SM in the snow area is very low. About 45% of the variability is caused by snow cover for SM. Snow cover area is mainly dependent on air temperature and the amount of precipitation and solid precipitation weaken the correlation. Snowfall reduces the absorbed solar radiation which decreases the energy absorbed from the sun. Generally, the snowfall occurs in highland sites. Although snow accumulation occurs in large percent, little of the moisture is released through snow melting. Rapid snow melting makes the runoff of water due to high land. So, this decreases the SMI in snow areas.

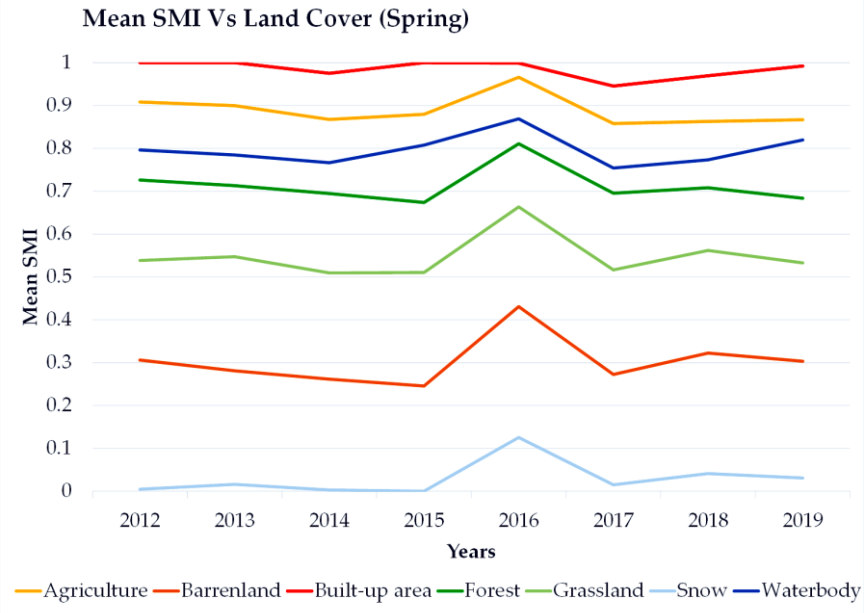

Figure 14. Mean SMI vs Land Cover (spring).

In figure 14, the SMI is high in the year 2016. This is because, in 2016 Spring, the rainfall was high than in other years.

3.6. Variation of Mean SMI with geographical region

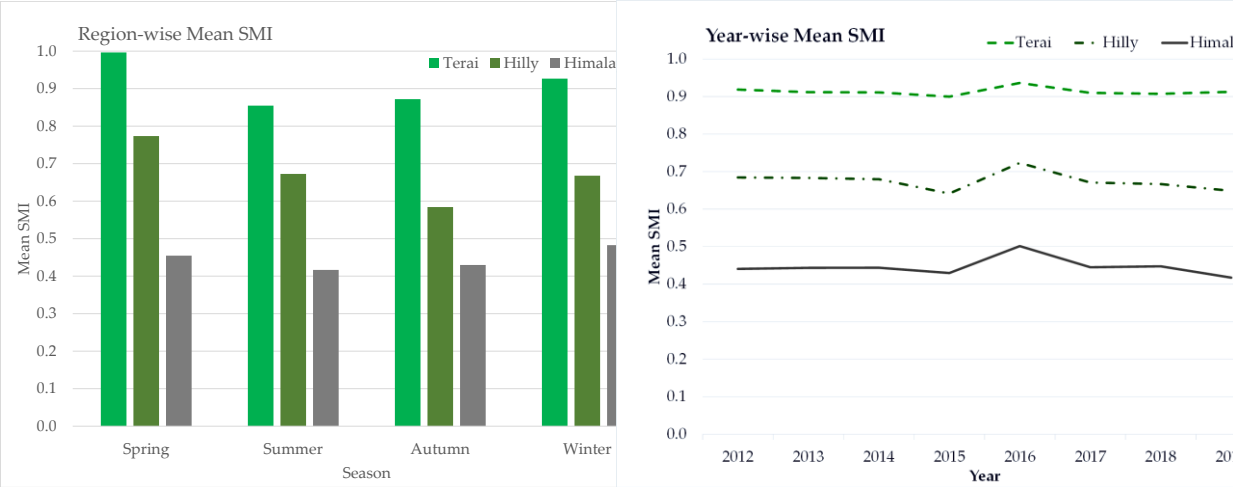

(**a**) (**b**)

Figure 15. Region-wise Mean SMI (**a**) Season-wise and (**b**) Year-wise.

There is a variation of SMI according to the season and year as shown in Figure 15(a) and (b) respectively. The SMI was high in spring and low in the autumn season in the Terai and the Hilly region. In the case of the Himalayan region, SMI was high in winter and low in the summer season. The SMI was generally high in comparison in the Terai region and low in the Himalayan region throughout the year. This result is in agreement with Roxy et al. [35].

3.7. Relationship between SMI and rainfall across Nepal

A year-wise study from 2012 to 2020 was carried out to observe the relationship between rainfall and SMI. As rainfall can directly impact the SM, it can show a clearer analysis of its relationship. In Nepal, the lowest rainfall was in winter (December-February) with 22mm rainfall on average all across Nepal and there is an increase in the rainfall as spring comes. The highest rainfall was observed in the summer (June-August) with the rainfall being 330mm on average all across Nepal. The graph of rainfall and SMI between the various seasons shows the gradual change except for 2016 where both SM and rainfall seem higher. In the graph mentioned below, the Correlation coefficient is 0.38 for autumn, 0.42 for spring, 0.31 for winter, 0.45 for summer between SMI and rainfall of the autumn and spring shows that they are positively correlated as shown in Figure 16.

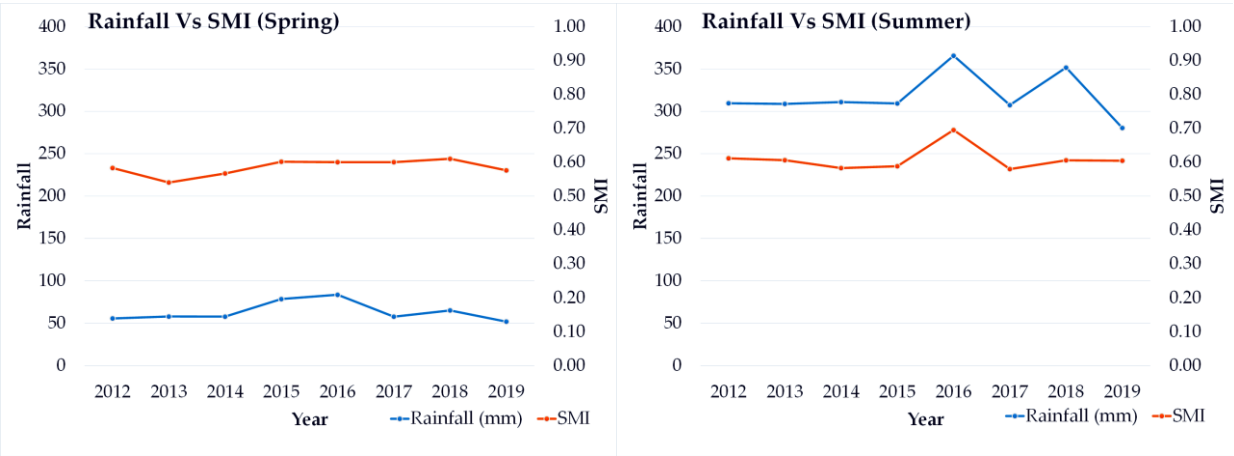

(**a**) (**b**)

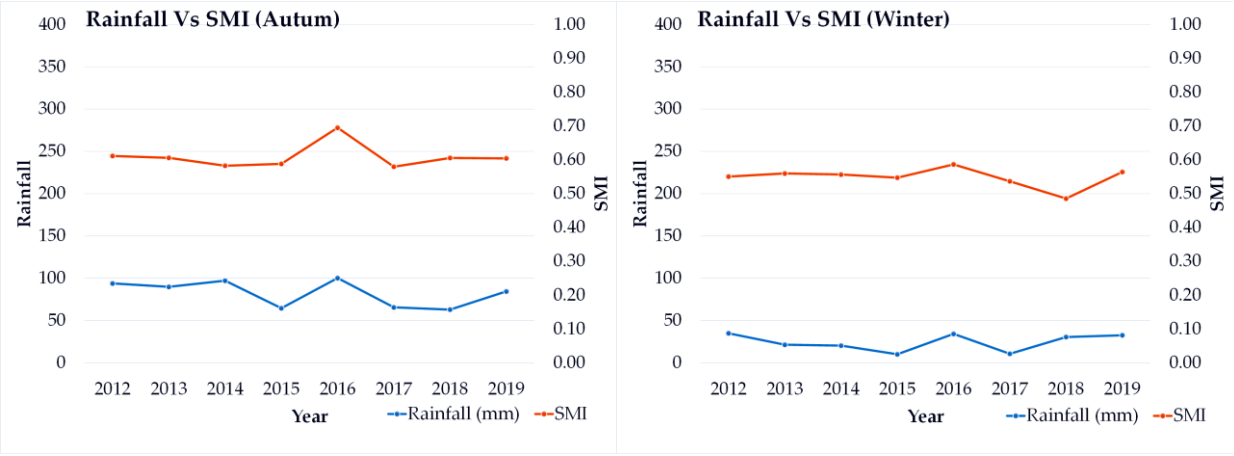

(**c**) (**d**)

Figure 16. Relationship of SMI with year and rainfall (**a**) SMI vs Rainfall (Spring), (**b**) SMI vs Rainfall (Summer), (**c**) SMI vs Rainfall (Autumn), and (**d**) SMI vs Rainfall (Winter).

The rainfall and SMI showed the befittingly direct relationship in almost all years in spring except for 2013 where rainfall is seemingly constant but SM has decreased. Likewise, in autumn the SMI and rainfall show direct relation in almost all years except 2014. These variations in these relations can be due to various factors affecting SM other than rainfall. In 2017 the rainfall in autumn on average all across Nepal is 63.05 mm which is decreased from the previous year's rainfall. The overall rainfall and SM are visibly decreased in the year 2017 for all seasons which also shows the positive relationship between SM and rainfall. The SMI generally follows rainfall patterns. But the SMI in the dune site did not show a significant relationship with the rainfall pattern.

3.8. Predicted SMI

After the validation of the predicted SMI map of 2020, the same model was used for predicting the SMI map of 2021(Figure 17). The maps show the gradual changes all across Nepal without any huge change. The eps-regression model used for the prediction of SMI values depicts that continuous data can be modelled, tested, and predicted with this version of the SVR model as the statistical analysis proved to be valuable to support the validation of predicted SMI values. For the actual and predicted SMI values of the spring season of the year 2020, RMSE was found to be 0.1045, which is less than 0.3, R- squared test was found to be 0.9485, which is closer to 1, MSE and MAE were found to be 0.0109 and 0.0884 respectively, which are both close to 0. Using this tested and validated model, the past calculated SMI values were used to predict the future SMI value.

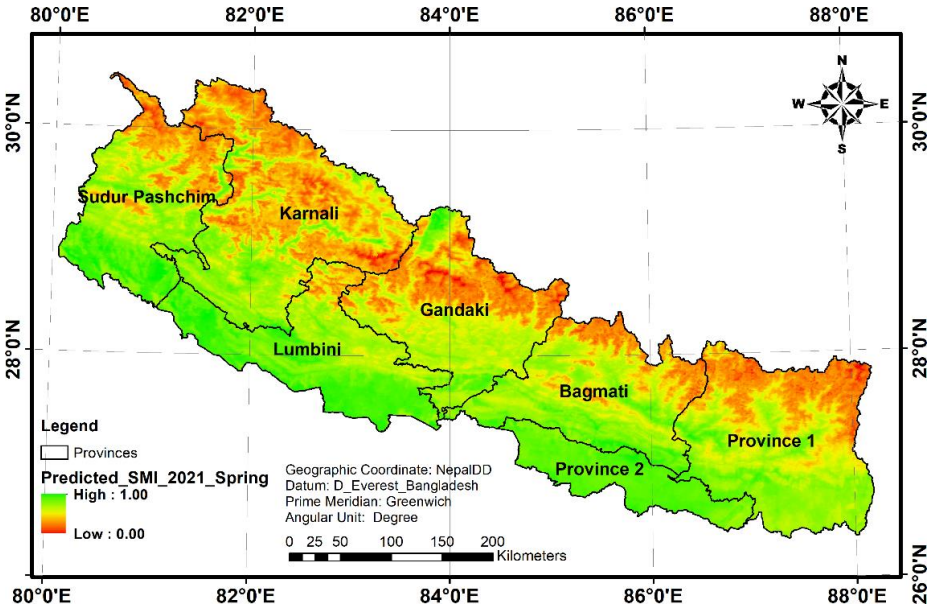

Figure 17. Predicted Soil Moisture Index (SMI) Map of Nepal (Spring 2021).

IV. Conclusion

The combination of NDVI and LST from MODIS data products is a useful tool for studying SM. Both LST and NDVI are dominant factors for SM influence. The analysis with significant NDVI, LST, and CHIRPS trends indicated that precipitation showed a positive impact on SMI at most places. NDVI was more susceptible to variations of rainfall. The SMI of the agricultural area is found to be more after built-up areas. This method is more appropriate for agricultural areas than for residential areas. SMI gradually decreases for water bodies, forests, grassland, barren land, and snow area which is reasonable according to Feng [34] research on SM.

Based on the overall result of this study, it can be concluded that SMI is high in Terai and low in the Himalayan region, and predicted SMI fits the previous pattern without rapid change in SM over regions. In the Terai and the Hilly region, the spring season has high SMI but in the Himalayan region, the winter season has high SMI. It also concludes that SMI is directly proportional to the rainfall amount. In 2016, due to high rainfall, the SMI of different land cover types was found to be high than in other years. These results can be useful to detect early signs of draught which can affect the agriculture and livelihood of the country's people. The seasonal distribution of SMI can be helpful to assess the needs of the irrigational facility, choice of crops and their rotations, and finally to design a cropping calendar. The potential crop/vegetation suitability maps could be prepared using the information of SMI. The SMI map produced can serve as a valuable basis for the upcoming studies and research exploring the effects of change in agricultural practice.

We had to deal with certain challenges when doing the study. Working amid the COVID-19 pandemic and lockdown had influenced our resources and time for this study. Insitu measurement was not possible for the validation for which we had to depend on the secondary data. Because of the coarse resolution of MODIS data, no comparisons between ground observations and RS-based results were undertaken in this study. This study is based solely on LST and NDVI values as they bear a strong relationship with the SM. It is recommended to consider factors other than temperature and vegetation that directly impacts the SM like topography, soil type, and others. If those factors are taken into account, additional findings will be obtained. As we have considered the whole of Nepal as our study area, it gives more generalized data which can be only of little use when examining a small area. Land use plays an important role in controlling spatial and temporal variations of SM by influencing infiltration rates, runoff, and evapotranspiration, which is important to crop growth and vegetation restoration. Therefore, SMI taking the consideration of land use can be more advantageous. The elevation is a factor that also plays a major role in estimating SMI value. As our country possesses a wide spectrum of topography, the elevation of land cover can also be taken into account.

Author Contributions: Conceptualization, Bhawana Baniya, Amit Tiwari, Ashish Dutta and Prajwol K.C.; Data curation, Bhawana Baniya, Amit Tiwari, Ashish Dutta and Prajwol K.C.; Formal analysis, Bhawana Baniya, Amit Tiwari, Ashish Dutta, Prajwol K.C., Pradeep Gyawali and Tri Acharya; Investigation, Bhawana Baniya; Methodology, Bhawana Baniya, Amit Tiwari, Ashish Dutta and Prajwol K.C.; Software, Amit Tiwari, Prajwol K.C. and Tri Acharya; Supervision, Pradeep Gyawali and Tri Acharya; Validation, Prajwol K.C.; Visualization, Prajwol K.C., Pradeep Gyawali and Tri Acharya; Writing – original draft, Bhawana Baniya, Amit Tiwari and Ashish Dutta; Writing – review & editing, Tri Acharya. All authors have read and agreed to the published version of the manuscript.

Funding: This research received no external funding.
Data Availability Statement: All data are available in USGS EarthExplore and EarthData.

Acknowledgements: We acknowledge the free availability of data via USGS and EarthData. The work is a result of an undergraduate thesis supervised by Kushal Sharma and Pawan Thapa from the Department of Geomatics Engineering, Kathmandu University Nepal. The manuscript was prepared via the #Mentor4Nepal Initiative (https://github.com/trydave/Mentor4Nepal).

Conflicts of Interest: The authors declare no conflict of interest.

References

[1]. DOA Inter Provincial Dependency for Agricultural Development. *Minist. Agric. L. Manag. Coop.* **2018**.
[2]. Chaudhary, D. Agricultural Policies and Rural Development in Nepal: An Overview. *Res. Nepal J. Dev. Stud.* **2018**, *1*, 34–46, doi:10.3126/rnjds.v1i2.22425.
[3]. Ghimire, Y.N.; Shivakoti, G.P.; Perret, S.R. Household-level vulnerability to drought in hill agriculture of Nepal: implications for adaptation planning. *Int. J. Sustain. Dev. \& World Ecol.* **2010**, *17*, 225–230, doi:10.1080/13504501003737500.
[4]. Gauchan, D. Agricultural Development in Nepal : Emerging Challenges and Opportunities. *Discourses Nepal's Dev. (Volume I)* **2018**, *2*, 212–240.
[5]. Malla, G. Climate Change and Its Impact on Nepalese Agriculture. *J. Agric. Environ.* **2009**, *9*, 62–71, doi:10.3126/aej.v9i0.2119.
[6]. KC, A.; Acharya, T.D.; Wagle, N.; Lee, D.H. Tracking Long-term Phenological Shift in Response to Climatic Parameters in Chitwan National Park, Nepal. *Sensors Mater.* **2021**, *33*, x, doi:10.18494/SAM.2021.3449.

[7]. Xu, Y.; Wang, L.; Ross, K.W.; Liu, C.; Berry, K. Standardized soil moisture index for drought monitoring based on soil moisture active passive observations and 36 years of North American Land Data Assimilation System data: A case study in the Southeast United States. *Remote Sens.* **2018**, *10*, doi:10.3390/rs10020301.

[8]. Son, N.T.; Chen, C.F.; Chen, C.R.; Chang, L.Y.; Minh, V.Q. Monitoring agricultural drought in the Lower Mekong Basin using MODIS NDVI and land surface temperature data. *Int. J. Appl. Earth Obs. Geoinf.* **2012**, *18*, 417–427, doi:10.1016/j.jag.2012.03.014.

[9]. Han, Y.; Wang, Y.; Zhao, Y. Estimating soil moisture conditions of the greater changbai mountains by land surface temperature and ndvi. *IEEE Trans. Geosci. Remote Sens.* **2010**, *48*, 2509–2515, doi:10.1109/TGRS.2010.2040830.

[10]. Saha, A.; Patil, M.; Goyal, V.C.; Rathore, D.S. Assessment and Impact of Soil Moisture Index in Agricultural Drought Estimation Using Remote Sensing and GIS Techniques. *Proceedings* **2018**, *7*, 2, doi:10.3390/ecws-3-05802.

[11]. Taktikou, E.; Bourazanis, G.; Papaioannou, G.; Kerkides, P. Prediction of Soil Moisture from Remote Sensing Data. *Procedia Eng.* **2016**, *162*, 309–316, doi:10.1016/j.proeng.2016.11.066.

[12]. Carlson, T. An overview of the "triangle method" for estimating surface evapotranspiration and soil moisture from satellite imagery. *Sensors* **2007**, *7*, 1612–1629, doi:10.3390/s7081612.

[13]. Wang, L.; Qu, J.J.; Zhang, S.; Hao, X.; Dasgupta, S. Soil moisture estimation using MODIS and ground measurements in Eastern China. *Int. J. Remote Sens.* **2007**, *28*, 1413–1418, doi:10.1080/01431160601075525.

[14]. Carlson, T.N.; Gillies, R.R.; Perry, E.M. A method to make use of thermal infrared temperature and NDVI measurements to infer surface soil water content and fractional vegetation cover. *Remote Sens. Rev.* **1994**, *9*, 161–173, doi:10.1080/02757259409532220.

[15]. Xu, C.; Qu, J.J.; Hao, X.; Cosh, M.H.; Prueger, J.H.; Zhu, Z.; Gutenberg, L. Downscaling of surface soil moisture retrieval by combining MODIS/Landsat and in situ measurements. *Remote Sens.* **2018**, *10*, doi:10.3390/rs10020210.

[16]. Lai, S.; Serra, M. Concrete strength prediction by means of neural network. *Constr. Build. Mater.* **1997**, *11*, 93–98, doi:10.1016/S0950-0618(97)00007-X.

[17]. Vembandasamy, K.; Sasipriya, R.; Deepa, E. Heart Diseases Detection Using Naive Bayes Algorithm. *Int. J. Innov. Sci. Eng. Technol.* **2015**, *2*, 441–444.

[18]. Cherkassky, V.; Ma, Y. Practical selection of SVM parameters and noise estimation for SVM regression. *Neural Networks* **2004**, *17*, 113–126, doi:https://doi.org/10.1016/S0893-6080(03)00169-2.

[19]. O. Akande, K.; O. Owolabi, T.; Twaha, S.; Olatunji, S.O. Performance Comparison of SVM and ANN in Predicting Compressive Strength of Concrete. *IOSR J. Comput. Eng.* **2014**, *16*, 88–94, doi:10.9790/0661-16518894.

[20]. Gupta, S.M. Support Vector Machines based Modelling of Concrete Strength. *World Acad. Sci. Eng. Technol.* **2007**, *36*, 305–311.

[21]. Justice, C.O.; Townshend, J.R.G.; Vermote, E.F.; Masuoka, E.; Wolfe, R.E.; Saleous, N.; Roy, D.P.; Morisette, J.T. An overview of MODIS Land data processing and product status. *Remote Sens. Environ.* **2002**, *83*, 3–15, doi:https://doi.org/10.1016/S0034-4257(02)00084-6.

[22]. Gandhi, G.M.; Parthiban, S.; Thummalu, N.; Christy, A. Ndvi: Vegetation Change Detection Using Remote Sensing and GIS – A Case Study of Vellore District. *Procedia Comput. Sci.* **2015**, *57*, 1199–1210, doi:https://doi.org/10.1016/j.procs.2015.07.415.

[23]. Bellón, B.; Bégué, A.; Lo Seen, D.; de Almeida, C.; Simões, M. A Remote Sensing Approach for Regional-Scale Mapping of Agricultural Land-Use Systems Based on NDVI Time Series. *Remote Sens.* **2017**, *9*, 600, doi:10.3390/rs9060600.

[24]. Zhang, F.; Tiyip, T.; Kung, H.; Johnson, V.C.; Maimaitiyiming, M.; Zhou, M.; Wang, J. Dynamics of land surface temperature (LST) in response to land use and land cover (LULC) changes in the Weigan and Kuqa river oasis, Xinjiang, China. *Arab. J. Geosci.* **2016**, *9*, 499, doi:10.1007/s12517-016-2521-8.

[25]. Prata, A.J.; Caselles, V.; Coll, C.; Sobrino, J.A.; Ottlé, C. Thermal remote sensing of land surface temperature from satellites: Current status and future prospects. *Remote Sens. Rev.* **1995**, *12*, 175–224, doi:10.1080/02757259509532285.

[26]. Buchhorn, M.; Smets, B.; Bertels, L.; Lesiv, M.; Tsendbazar, N.-E.; Masiliunas, D.; Linlin, L.; Herold, M.; Fritz, S. Copernicus Global Land Service: Land Cover 100m: collection 3: epoch 2019: Globe (V3.0.1) [Data set] Available online: https://zenodo.org/record/3939050 (accessed on Nov 19, 2020).

[27]. Luo, X.; Wu, W.; He, D.; Li, Y.; Ji, X. Hydrological Simulation Using TRMM and CHIRPS Precipitation Estimates in the Lower Lancang-Mekong River Basin. *Chinese Geogr. Sci.* **2019**, *29*, 13–25, doi:10.1007/s11769-019-1014-6.

[28]. Ghozat, A.; Sharafati, A.; Hosseini, S.A. Long-term spatiotemporal evaluation of CHIRPS satellite precipitation product over different climatic regions of Iran. *Theor. Appl. Climatol.* **2021**, *143*, 211–225, doi:10.1007/s00704-020-03428-5.

[29]. Chauhan, N.S.; Miller, S.; Ardanuy, P. Spaceborne soil moisture estimation at high resolution: a microwave-optical/IR synergistic approach. *Int. J. Remote Sens.* **2003**, *24*, 4599–4622, doi:10.1080/0143116031000156837.

[30]. Li, X.; Lord, D.; Zhang, Y.; Xie, Y. Predicting motor vehicle crashes using Support Vector Machine models. *Accid. Anal. Prev.* **2008**, *40*, 1611–1618, doi:10.1016/j.aap.2008.04.010.

[31]. Kecman, V. Support Vector Machines -- An Introduction. In *Support Vector Machines: Theory and Applications*; Wang, L., Ed.; Springer Berlin Heidelberg: Berlin, Heidelberg, 2005; pp. 1–47 ISBN 978-3-540-32384-6.

[32]. Pasolli, L.; Notarnicola, C.; Bruzzone, L. Estimating Soil Moisture With the Support Vector Regression Technique. *IEEE Geosci. Remote Sens. Lett.* **2011**, *8*, 1080–1084, doi:10.1109/LGRS.2011.2156759.

[33]. Kashif Gill, M.; Kemblowski, M.W.; McKee, M. Soil Moisture Data Assimilation Using Support Vector Machines and Ensemble Kalman Filter. *J. Am. Water Resour. Assoc.* **2007**, *43*, 1004–1015, doi:10.1111/j.1752-1688.2007.00082.x.

[34]. Feng, H.; Liu, Y. Combined effects of precipitation and air temperature on soil moisture in different land covers in a humid basin. *J. Hydrol.* **2015**, *531*, 1129–1140, doi:https://doi.org/10.1016/j.jhydrol.2015.11.016.

[35]. Roxy, M.S.; Sumithranand, V.B.; Renuka, G. Variability of soil moisture and its relationship with surface albedo and soil thermal diffusivity at Astronomical Observatory, Thiruvananthapuram, South Kerala. *J. Earth Syst. Sci.* **2010**, *119*, 507–517, doi:10.1007/s12040-010-0038-1.